Review | Vol. 26, No. 19 | 17 Sep 2018 | OPTICS EXPRESS 24531
Optics EXPRESS

Photonics meets topology

BI-YE XIE,[1] HONG-FEI WANG,[1] XUE-YI ZHU,[1] MING-HUI LU,[1,3,4,*] Z. D. WANG,[2] AND YAN-FENG CHEN,[1,3]

[1]National Laboratory of Solid State Microstructures and Department of Materials Science and Engineering, Nanjing University, Nanjing 210093, China
[2]Department of Physics and Center of Theoretical and Computational Physics, The University of Hong Kong, Pokfulam Road, Hong Kong, China
[3]Jiangsu Key Lab. of Artificial Functional Materials, Nanjing University, Nanjing 210093, China
[4]Collaborative Innovation Center of Advanced Microstructures, Nanjing University, Nanjing 210093, China
[*]luminghui@nju.edu.cn

Abstract: The topological phases in materials have been studied in recent decades for their unique boundary states and transport properties. Photonic systems with band structures embrace the topological phases closely, where they not only provide platforms to testify the topological band theory, but also shed light on designing novel optical devices. In this review, we present exciting developments, supported by brief descriptions of prominent milestones of topological phases in photonic systems in recent years. These studies may sustain further developments of optical devices and offer novel methods for light manipulations.

OCIS codes: (160.0160) Materials, (130.5296) Photonic crystal waveguides, (160.5293) Photonic bandgap materials

References and links

1. P. W. Anderson, "More is different," Science **177**(4047), 393–396 (1972).
2. J. D. Joannopoulos, S. G. Johnson, J. N. Winn, and R. D. Meade, *Photonic crystals: molding the flow of light* (Princeton university press, 2011).
3. E. Yablonovitch, "Inhibited spontaneous emission in solid-state physics and electronics," Phys. Rev. Lett. **58**(20), 2059–2062 (1987).
4. S. John, "Strong localization of photons in certain disordered dielectric superlattices," Phys. Rev. Lett. **58**(23), 2486–2489 (1987).
5. A. Yariv, Y. Xu, R. K. Lee, and A. Scherer, "Coupled-resonator optical waveguide: a proposal and analysis," Opt. Lett. **24**(11), 711–713 (1999).
6. C. M. Soukoulis and M. Wegener, "Past achievements and future challenges in the development of three-dimensional photonic metamaterials," Nat. Photonics **5**(9), 523–530 (2011).
7. M. Z. Hasan and C. L. Kane, "Colloquium: Topological insulators," Rev. Mod. Phys. **82**(4), 3045–3067 (2010).
8. X. L. Qi and S. C. Zhang, "Topological insulators and superconductors," Rev. Mod. Phys. **83**(4), 1057–1110 (2011).
9. A. Bansil, H. Lin, and T. Das, "Colloquium: Topological band theory," Rev. Mod. Phys. **88**(2), 021004 (2016).
10. K. V. Klitzing, G. Dorda, and M. Pepper, "New Method for High-Accuracy Determination of the Fine-Structure Constant Based on Quantized Hall Resistance," Phys. Rev. Lett. **45**(6), 494–497 (1980).
11. C. X. Liu, S. C. Zhang, and X. L. Qi, "The Quantum anomalous Hall effect: theory and experiment," Annu. Rev. Condens. Matter Phys. **7**(1), 301–321 (2016).
12. C. L. Kane and E. J. Mele, "Quantum spin Hall effect in graphene," Phys. Rev. Lett. **95**(22), 226801 (2005).
13. D. J. Thouless, M. Kohmoto, M. P. Nightingale, and M. den Nijs, "Quantized Hall conductance in a two-dimensional periodic potential," Phys. Rev. Lett. **49**(6), 405–408 (1982).
14. C. He, X. Ni, H. Ge, X. C. Sun, Y.-B. Chen, M.-H. Lu, X.-P. Liu, and Y.-F. Chen, "Acoustic topological insulator and robust one-way sound transport," Nat. Phys. **12**(12), 1124–1129 (2016).
15. A. Karch, "Surface plasmons and topological insulators," Phys. Rev. B **83**(24), 245432 (2011).
16. S. D. Huber, "Topological mechanics," Nat. Phys. **12**(7), 621–623 (2016).
17. C. K. Chiu, J. C. Y. Teo, A. P. Schnyder, and S. Ryu, "Classification of topological quantum matter with symmetries," Rev. Mod. Phys. **88**(3), 035005 (2016).
18. S. Ryu, A. P. Schnyder, A. Furusaki, and A. W. Ludwig, "Topological insulators and superconductors: tenfold way and dimensional hierarchy," New J. Phys. **12**(6), 065010 (2010).
19. C. K. Chiu, H. Yao, and S. Ryu, "Classification of topological insulators and superconductors in the presence of reflection symmetry," Phys. Rev. B **88**(7), 075142 (2013).
20. T. Morimoto and A. Furusaki, "Topological classification with additional symmetries from Clifford algebras," Phys. Rev. B **88**(12), 125129 (2013).
21. C. Fang, M. J. Gilbert, and B. A. Bernevig, "Bulk topological invariants in noninteracting point group symmetric insulators," Phys. Rev. B **86**(11), 115112 (2012).

#337603 https://doi.org/10.1364/OE.26.024531
Journal © 2018 Received 6 Jul 2018; accepted 20 Aug 2018; published 5 Sep 2018

Optics EXPRESS

22. R. J. Slager, A. Mesaros, V. Juričić, and J. Zaanen, "The space group classification of topological band-insulators," Nat. Phys. **9**(2), 98–102 (2013).
23. K. Shiozaki and M. Sato, "Topology of crystalline insulators and superconductors," Phys. Rev. B **90**(16), 165114 (2014).
24. F. Nathan and M. S. Rudner, "Topological singularities and the general classification of Floquet–Bloch systems," New J. Phys. **17**(12), 125014 (2015).
25. F. S. Nathan, *Topological Classification of Floquet-Bloch Systems* (Niels Bohr Institute, Copenhagen University, 2015).
26. K. Shiozaki, M. Sato, and K. Gomi, "Topology of nonsymmorphic crystalline insulators and superconductors," Phys. Rev. B **93**(19), 195413 (2016).
27. S. Raghu and F. Haldane, "Analogs of quantum-Hall-effect edge states in photonic crystals," Phys. Rev. A **78**(3), 033834 (2008).
28. M. R. Zirnbauer, "Riemannian symmetric superspaces and their origin in random-matrix theory," J. Math. Phys. **37**(10), 4986–5018 (1996).
29. A. Altland and M. R. Zirnbauer, "Nonstandard symmetry classes in mesoscopic normal-superconducting hybrid structures," Phys. Rev. B **55**(2), 1142–1161 (1997).
30. Z. Wang, Y. D. Chong, J. D. Joannopoulos, and M. Soljacić, "Reflection-free one-way edge modes in a gyromagnetic photonic crystal," Phys. Rev. Lett. **100**(1), 013905 (2008).
31. Z. Wang, Y. Chong, J. D. Joannopoulos, and M. Soljacić, "Observation of unidirectional backscattering-immune topological electromagnetic states," Nature **461**(7265), 772–775 (2009).
32. K. Liu, L. Shen, and S. He, "One-way edge mode in a gyromagnetic photonic crystal slab," Opt. Lett. **37**(19), 4110–4112 (2012).
33. X. Ao, Z. Lin, and C. Chan, "One-way edge mode in a magneto-optical honeycomb photonic crystal," Phys. Rev. B **80**(3), 033105 (2009).
34. Z. Li, R. X. Wu, Q. B. Li, and Y. Poo, "Realization of self-guided unidirectional waveguides by a chain of gyromagnetic rods," Appl. Opt. **54**(6), 1267–1272 (2015).
35. S. A. Skirlo, L. Lu, and M. Soljačić, "Multimode one-way waveguides of large Chern numbers," Phys. Rev. Lett. **113**(11), 113904 (2014).
36. S. A. Skirlo, L. Lu, Y. Igarashi, Q. Yan, J. Joannopoulos, and M. Soljačić, "Experimental observation of large chern numbers in photonic crystals," Phys. Rev. Lett. **115**(25), 253901 (2015).
37. S. Mansha and Y. Chong, "Robust edge states in amorphous gyromagnetic photonic lattices," Phys. Rev. B **96**(12), 121405 (2017).
38. M. Xiao and S. Fan, "Photonic Chern insulator through homogenization of an array of particles," Phys. Rev. B **96**(10), 100202 (2017).
39. K. Fang, Z. Yu, and S. Fan, "Microscopic theory of photonic one-way edge mode," Phys. Rev. B **84**(7), 075477 (2011).
40. A. A. Asatryan, L. C. Botten, K. Fang, S. Fan, and R. C. McPhedran, "Local density of states of chiral Hall edge states in gyrotropic photonic clusters," Phys. Rev. B **88**(3), 035127 (2013).
41. C. He, X. C. Sun, X. P. Liu, M. H. Lu, Y. Chen, L. Feng, and Y.-F. Chen, "Photonic topological insulator with broken time-reversal symmetry," Proc. Natl. Acad. Sci. U.S.A. **113**(18), 4924–4928 (2016).
42. D. A. Jacobs, A. E. Miroshnichenko, Y. S. Kivshar, and A. B. Khanikaev, "Photonic topological Chern insulators based on Tellegen metacrystals," New J. Phys. **17**(12), 125015 (2015).
43. T. Ochiai, "Time-reversal-violating photonic topological insulators with helical edge states," J. Phys. Soc. Jpn. **84**(5), 054401 (2015).
44. X. C. Sun, C. He, X. P. Liu, M. H. Lu, S. N. Zhu, and Y. F. Chen, "Two-dimensional topological photonic systems," Prog. Quantum Electron. **55**, 52–73 (2017).
45. C. He, X. L. Chen, M. H. Lu, X. F. Li, W. W. Wan, X. S. Qian, R. C. Yin, and Y. F. Chen, "Tunable one-way cross-waveguide splitter based on gyromagnetic photonic crystal," Appl. Phys. Lett. **96**(11), 111111 (2010).
46. C. He, X. L. Chen, M. H. Lu, X. F. Li, W. W. Wan, X. S. Qian, R. C. Yin, and Y. F. Chen, "Left-handed and right-handed one-way edge modes in a gyromagnetic photonic crystal," J. Appl. Phys. **107**(12), 123117 (2010).
47. S. Liu, W. Lu, Z. Lin, and S. Chui, "Magnetically controllable unidirectional electromagnetic waveguiding devices designed with metamaterials," Appl. Phys. Lett. **97**(20), 201113 (2010).
48. Z. Wang, L. Shen, Z. Yu, X. Zhang, and X. Zheng, "Highly efficient photonic-crystal splitters based on one-way waveguiding," JOSA B **30**(1), 173–176 (2013).
49. X. Zang and C. Jiang, "Edge mode in nonreciprocal photonic crystal waveguide: manipulating the unidirectional electromagnetic pulse dynamically," JOSA B **28**(3), 554–557 (2011).
50. Z. Wang, L. Shen, X. Zhang, Y. Wang, Z. Yu, and X. Zheng, "Photonic crystal cavity with one-way rotating state and its coupling with photonic crystal waveguide," J. Appl. Phys. **110**(4), 043106 (2011).
51. W. Qiu, Z. Wang, and M. Soljačić, "Broadband circulators based on directional coupling of one-way waveguides," Opt. Express **19**(22), 22248–22257 (2011).
52. L. Zhang, D. Yang, K. Chen, T. Li, and S. Xia, "Design of nonreciprocal waveguide devices based on two-dimensional magneto-optical photonic crystals," Opt. Laser Technol. **50**, 195–201 (2013).
53. B. Bahari, R. Tellez-Limon, and B. Kanté, "Topological terahertz circuits using semiconductors," Appl. Phys. Lett. **109**(14), 143501 (2016).
54. D. Wang, C. Qiu, P. T. Rakich, and Z. Wang, "Guide-wave photonic pulling force using one-way photonic chiral edge states," in *CLEO: QELS_Fundamental Science*, (Optical Society of America, 2015), FM2D. 7.
55. M. Hafezi and P. Rabl, "Optomechanically induced non-reciprocity in microring resonators," Opt. Express **20**(7), 7672–7684 (2012).

Optics EXPRESS

56. M. C. Onbasli, L. Beran, M. Zahradník, M. Kučera, R. Antoš, J. Mistrík, G. F. Dionne, M. Veis, and C. A. Ross, "Optical and magneto-optical behavior of Cerium Yttrium Iron Garnet thin films at wavelengths of 200-1770 nm," Sci. Rep. **6**(1), 23640 (2016).
57. T. Ozawa, H. M. Price, A. Amo, N. Goldman, M. Hafezi, L. Lu, M. Rechtsman, D. Schuster, J. Simon, and O. Zilberberg, "Topological photonics," arXiv preprint arXiv:1802.04173 (2018)
58. A. B. Khanikaev and G. Shvets, "Two-dimensional topological photonics," Nat. Photonics **11**(12), 763–773 (2017).
59. L. Lu, J. D. Joannopoulos, and M. Soljačić, "Topological photonics," Nat. Photonics **8**(11), 821–829 (2014).
60. M. Hafezi, E. A. Demler, M. D. Lukin, and J. M. Taylor, "Robust optical delay lines with topological protection," Nat. Phys. **7**(11), 907–912 (2011).
61. M. Hafezi, S. Mittal, J. Fan, A. Migdall, and J. Taylor, "Imaging topological edge states in silicon photonics," Nat. Photonics **7**(12), 1001–1005 (2013).
62. K. Y. Bliokh, D. Smirnova, and F. Nori, "Quantum spin Hall effect of light," Science **348**(6242), 1448–1451 (2015).
63. K. Y. Bliokh, F. Rodríguez-Fortuño, F. Nori, and A. V. Zayats, "Spin–orbit interactions of light," Nat. Photonics **9**(12), 796–808 (2015).
64. A. B. Khanikaev, S. Hossein Mousavi, W.-K. Tse, M. Kargarian, A. H. MacDonald, and G. Shvets, "Photonic topological insulators," Nat. Mater. **12**(3), 233–239 (2013).
65. T. Ma, A. B. Khanikaev, S. H. Mousavi, and G. Shvets, "Guiding electromagnetic waves around sharp corners: topologically protected photonic transport in metawaveguides," Phys. Rev. Lett. **114**(12), 127401 (2015).
66. X. Cheng, C. Jouvaud, X. Ni, S. H. Mousavi, A. Z. Genack, and A. B. Khanikaev, "Robust reconfigurable electromagnetic pathways within a photonic topological insulator," Nat. Mater. **15**(5), 542–548 (2016).
67. K. Lai, T. Ma, X. Bo, S. Anlage, and G. Shvets, "Experimental realization of a reflections-free compact delay line based on a photonic topological insulator," Sci. Rep. **6**(1), 28453 (2016).
68. B. Xiao, K. Lai, Y. Yu, T. Ma, G. Shvets, and S. M. Anlage, "Exciting reflectionless unidirectional edge modes in a reciprocal photonic topological insulator medium," Phys. Rev. B **94**(19), 195427 (2016).
69. A. Slobozhanyuk, S. H. Mousavi, X. Ni, D. Smirnova, Y. S. Kivshar, and A. B. Khanikaev, "Three-dimensional all-dielectric photonic topological insulator," Nat. Photonics **11**(2), 130–136 (2017).
70. L. H. Wu and X. Hu, "Scheme for achieving a topological photonic crystal by using dielectric material," Phys. Rev. Lett. **114**(22), 223901 (2015).
71. Y. Yang, Y. F. Xu, T. Xu, H. X. Wang, J. H. Jiang, X. Hu, and Z. H. Hang, "Visualization of a Unidirectional Electromagnetic Waveguide Using Topological Photonic Crystals Made of Dielectric Materials," Phys. Rev. Lett. **120**(21), 217401 (2018).
72. M. S. Dresselhaus, G. Dresselhaus, and A. Jorio, *Group theory: application to the physics of condensed matter* (Springer Science & Business Media, 2007).
73. W.-K. Tse, Z. Qiao, Y. Yao, A. MacDonald, and Q. Niu, "Quantum anomalous Hall effect in single-layer and bilayer graphene," Phys. Rev. B **83**(15), 155447 (2011).
74. F. Guinea, M. Katsnelson, and A. Geim, "Energy gaps and a zero-field quantum Hall effect in graphene by strain engineering," Nat. Phys. **6**(1), 30–33 (2010).
75. M. Ezawa, "Valley-polarized metals and quantum anomalous Hall effect in silicene," Phys. Rev. Lett. **109**(5), 055502 (2012).
76. H. Pan, Z. Li, C.-C. Liu, G. Zhu, Z. Qiao, and Y. Yao, "Valley-polarized quantum anomalous Hall effect in silicene," Phys. Rev. Lett. **112**(10), 106802 (2014).
77. F. Gao, H. Xue, Z. Yang, K. Lai, Y. Yu, X. Lin, Y. Chong, G. Shvets, and B. Zhang, "Topologically protected refraction of robust kink states in valley photonic crystals," Nat. Phys. **14**(2), 140–144 (2017).
78. Y. Yang, H. Jiang, and Z. H. Hang, "Topological Valley Transport in Two-dimensional Honeycomb Photonic Crystals," Sci. Rep. **8**(1), 1588 (2018).
79. X. Ni, D. Purtseladze, D. A. Smirnova, A. Slobozhanyuk, A. Alù, and A. B. Khanikaev, "Spin- and valley-polarized one-way Klein tunneling in photonic topological insulators," Sci. Adv. **4**(5), eaap8802 (2018).
80. Y. Kang, X. Cheng, X. Ni, A. B. Khanikaev, and A. Z. Genack, "Pseudospin-valley coupled edge states in a photonic topological insulator," arXiv preprint arXiv:1804.08707 (2018).
81. J. Ningyuan, C. Owens, A. Sommer, D. Schuster, and J. Simon, "Time-and site-resolved dynamics in a topological circuit," Phys. Rev. X **5**(2), 021031 (2015).
82. N. Schine, A. Ryou, A. Gromov, A. Sommer, and J. Simon, "Synthetic Landau levels for photons," Nature **534**(7609), 671–675 (2016).
83. L. Lu, C. Fang, L. Fu, S. G. Johnson, J. D. Joannopoulos, and M. Soljačić, "Symmetry-protected topological photonic crystal in three dimensions," Nat. Phys. **12**(4), 337–340 (2016).
84. L. Fu, "Topological crystalline insulators," Phys. Rev. Lett. **106**(10), 106802 (2011).
85. F. Liu, H. Y. Deng, and K. Wakabayashi, "Topological photonic crystals with zero Berry curvature," Phys. Rev. B **97**(3), 035442 (2018).
86. F. Liu and K. Wakabayashi, "Novel topological phase with a zero Berry curvature," Phys. Rev. Lett. **118**(7), 076803 (2017).
87. Y. Zhao and A. P. Schnyder, "Nonsymmorphic symmetry-required band crossings in topological semimetals," Phys. Rev. B **94**(19), 195109 (2016).
88. D. Varjas, F. de Juan, and Y. M. Lu, "Bulk invariants and topological response in insulators and superconductors with nonsymmorphic symmetries," Phys. Rev. B **92**(19), 195116 (2015).
89. S. M. Young and C. L. Kane, "Dirac semimetals in two dimensions," Phys. Rev. Lett. **115**(12), 126803 (2015).

Optics EXPRESS

90. K. Shiozaki, M. Sato, and K. Gomi, "Z 2 topology in nonsymmorphic crystalline insulators: Möbius twist in surface states," Phys. Rev. B **91**(15), 155120 (2015).
91. J. Cayssol, B. Dóra, F. Simon, and R. Moessner, ""Floquet topological insulators," physica status solidi (RRL)-," Rapid Research Letters **7**(12), 101–108 (2013).
92. M. C. Rechtsman, J. M. Zeuner, Y. Plotnik, Y. Lumer, D. Podolsky, F. Dreisow, S. Nolte, M. Segev, and A. Szameit, "Photonic Floquet topological insulators," Nature **496**(7444), 196–200 (2013).
93. M. S. Rudner, N. H. Lindner, E. Berg, and M. Levin, "Anomalous edge states and the bulk-edge correspondence for periodically driven two-dimensional systems," Phys. Rev. X **3**(3), 031005 (2013).
94. S. Mukherjee, A. Spracklen, M. Valiente, E. Andersson, P. Öhberg, N. Goldman, and R. R. Thomson, "Experimental observation of anomalous topological edge modes in a slowly driven photonic lattice," Nat. Commun. **8**, 13918 (2017).
95. Y. X. Zhao and Z. D. Wang, "Topological classification and stability of Fermi surfaces," Phys. Rev. Lett. **110**(24), 240404 (2013).
96. G. E. Volovik, *The universe in a helium droplet* (Oxford University Press on Demand, 2003), Vol. 117.
97. Y. Zhao and Z. Wang, "Topological connection between the stability of Fermi surfaces and topological insulators and superconductors," Phys. Rev. B **89**(7), 075111 (2014).
98. Y. X. Zhao, A. P. Schnyder, and Z. D. Wang, "Unified Theory of PT and CP Invariant Topological Metals and Nodal Superconductors," Phys. Rev. Lett. **116**(15), 156402 (2016).
99. R. Sepkhanov, Y. B. Bazaliy, and C. Beenakker, "Extremal transmission at the Dirac point of a photonic band structure," Phys. Rev. A **75**(6), 063813 (2007).
100. X. Wan, A. M. Turner, A. Vishwanath, and S. Y. Savrasov, "Topological semimetal and Fermi-arc surface states in the electronic structure of pyrochlore iridates," Phys. Rev. B **83**(20), 205101 (2011).
101. A. A. Burkov and L. Balents, "Weyl semimetal in a topological insulator multilayer," Phys. Rev. Lett. **107**(12), 127205 (2011).
102. S. Y. Xu, I. Belopolski, N. Alidoust, M. Neupane, G. Bian, C. Zhang, R. Sankar, G. Chang, Z. Yuan, C. C. Lee, S. M. Huang, H. Zheng, J. Ma, D. S. Sanchez, B. Wang, A. Bansil, F. Chou, P. P. Shibayev, H. Lin, S. Jia, and M. Z. Hasan, "Discovery of a Weyl fermion semimetal and topological Fermi arcs," Science **349**(6248), 613–617 (2015).
103. B. Lv, H. Weng, B. Fu, X. Wang, H. Miao, J. Ma, P. Richard, X. Huang, L. Zhao, G. Chen, Z. Fang, X. Dai, T. Qian, and H. Ding, "Experimental discovery of Weyl semimetal TaAs," Phys. Rev. X **5**(3), 031013 (2015).
104. H. Weng, C. Fang, Z. Fang, B. A. Bernevig, and X. Dai, "Weyl semimetal phase in noncentrosymmetric transition-metal monophosphides," Phys. Rev. X **5**(1), 011029 (2015).
105. D. Friedan, "A proof of the Nielsen-Ninomiya theorem," Commun. Math. Phys. **85**(4), 481–490 (1982).
106. L. Lu, L. Fu, J. D. Joannopoulos, and M. Soljačić, "Weyl points and line nodes in gyroid photonic crystals," Nat. Photonics **7**(4), 294–299 (2013).
107. A. A. Soluyanov, D. Gresch, Z. Wang, Q. Wu, M. Troyer, X. Dai, and B. A. Bernevig, "Type-II Weyl semimetals," Nature **527**(7579), 495–498 (2015).
108. J. Bravo-Abad, L. Lu, L. Fu, H. Buljan, and M. Soljačić, "Weyl points in photonic-crystal superlattices," 2D Materials **2**(3), 034013 (2015).
109. W. Gao, M. Lawrence, B. Yang, F. Liu, F. Fang, B. Béri, J. Li, and S. Zhang, "Topological photonic phase in chiral hyperbolic metamaterials," Phys. Rev. Lett. **114**(3), 037402 (2015).
110. M. Xiao, Q. Lin, and S. Fan, "Hyperbolic Weyl point in reciprocal chiral metamaterials," Phys. Rev. Lett. **117**(5), 057401 (2016).
111. C. Liu, W. Gao, B. Yang, and S. Zhang, "Disorder-Induced Topological State Transition in Photonic Metamaterials," Phys. Rev. Lett. **119**(18), 183901 (2017).
112. T. Ochiai, "Floquet-Weyl and Floquet-topological-insulator phases in a stacked two-dimensional ring-network lattice," J. Phys. Condens. Matter **28**(42), 425501 (2016).
113. H. Wang, L. Zhou, and Y. Chong, "Floquet Weyl phases in a three-dimensional network model," Phys. Rev. B **93**(14), 144114 (2016).
114. M. L. Chang, M. Xiao, W. J. Chen, and C. T. Chan, "Multiple Weyl points and the sign change of their topological charges in woodpile photonic crystals," Phys. Rev. B **95**(12), 125136 (2017).
115. Z. Yang, M. Xiao, F. Gao, L. Lu, Y. Chong, and B. Zhang, "Weyl points in a magnetic tetrahedral photonic crystal," Opt. Express **25**(14), 15772–15777 (2017).
116. W. J. Chen, M. Xiao, and C. T. Chan, "Photonic crystals possessing multiple Weyl points and the experimental observation of robust surface states," Nat. Commun. **7**, 13038 (2016).
117. J. Noh, S. Huang, D. Leykam, Y. D. Chong, K. P. Chen, and M. C. Rechtsman, "Experimental observation of optical Weyl points and Fermi arc-like surface states," Nat. Phys. **13**(6), 611–617 (2017).
118. B. Yang, Q. Guo, B. Tremain, R. Liu, L. E. Barr, Q. Yan, W. Gao, H. Liu, Y. Xiang, and J. Chen, "Ideal Weyl points and helicoid surface states in artificial photonic crystal structures," Science (**11**), eaaq1221 (2018).
119. B. Yang, Q. Guo, B. Tremain, L. E. Barr, W. Gao, H. Liu, B. Béri, Y. Xiang, D. Fan, A. P. Hibbins, and S. Zhang, "Direct observation of topological surface-state arcs in photonic metamaterials," Nat. Commun. **8**(1), 97 (2017).
120. H. X. Wang, Y. Chen, Z. H. Hang, H. Y. Kee, and J. H. Jiang, "Type-II Dirac photons," npj Quantum Materials **2**(1), 54 (2017).
121. H. Wang, L. Xu, H. Chen, and J. H. Jiang, "Three-dimensional photonic Dirac points stabilized by point group symmetry," Phys. Rev. B **93**(23), 235155 (2016).
122. A. Burkov, M. Hook, and L. Balents, "Topological nodal semimetals," Phys. Rev. B **84**(23), 235126 (2011).

Optics EXPRESS

123. L. Lu, L. Fu, J. D. Joannopoulos, and M. Soljačić, "Weyl points and line nodes in gyroid photonic crystals," Nat. Photonics **7**(4), 294–299 (2013).
124. C. Fang, H. Weng, X. Dai, and Z. Fang, "Topological nodal line semimetals," Chin. Phys. B **25**(11), 117106 (2016).
125. J. Y. Lin, N. C. Hu, Y. J. Chen, C. H. Lee, and X. Zhang, "Line nodes, Dirac points, and Lifshitz transition in two-dimensional nonsymmorphic photonic crystals," Phys. Rev. B **96**(7), 075438 (2017).
126. W. Gao, B. Yang, B. Tremain, H. Liu, Q. Guo, L. Xia, A. P. Hibbins, and S. Zhang, "Experimental observation of photonic nodal line degeneracies in metacrystals," Nat. Commun. **9**(1), 950 (2018).
127. T. Bzdušek, Q. Wu, A. Rüegg, M. Sigrist, and A. A. Soluyanov, "Nodal-chain metals," Nature **538**(7623), 75–78 (2016).
128. T. Kawakami and X. Hu, "Symmetry-Guaranteed and Accidental Nodal-Line Semimetals in FCC Lattice," arXiv preprint arXiv:1611.07342 (2016).
129. Q. Yan, R. Liu, Z. Yan, B. Liu, H. Chen, Z. Wang, and L. Lu, "Experimental discovery of nodal chains," Nat. Phys. **14**(5), 461–464 (2018).
130. Z. Yan, R. Bi, H. Shen, L. Lu, S. C. Zhang, and Z. Wang, "Nodal-link semimetals," Phys. Rev. B **96**(4), 041103 (2017).
131. R. Bi, Z. Yan, L. Lu, and Z. Wang, "Nodal-knot semimetals," Phys. Rev. B **96**(20), 201305 (2017).
132. G. Bian, T. R. Chang, H. Zheng, S. Velury, S. Y. Xu, T. Neupert, C. K. Chiu, S. M. Huang, D. S. Sanchez, I. Belopolski, N. Alidoust, P.-J. Chen, G. Chang, A. Bansil, H.-T. Jeng, H. Lin, and M. Z. Hasan, "Drumhead surface states and topological nodal-line fermions in TlTaSe 2," Phys. Rev. B **93**(12), 121113 (2016).
133. M. Xiao and S. Fan, "Topologically Charged Nodal Surface," arXiv preprint arXiv:1709.02363 (2017).
134. C. M. Bender and S. Boettcher, "Real spectra in non-Hermitian Hamiltonians having PT symmetry," Phys. Rev. Lett. **80**(24), 5243–5246 (1998).
135. S. Longhi, "Parity-time symmetry meets photonics: A new twist in non-Hermitian optics," EPL **120**(6), 64001 (2017).
136. R. El-Ganainy, K. G. Makris, M. Khajavikhan, Z. H. Musslimani, S. Rotter, and D. N. Christodoulides, "Non-Hermitian physics and PT symmetry," Nat. Phys. **14**(1), 11–19 (2018).
137. W. Heiss, "The physics of exceptional points," J. Phys. A Math. Theor. **45**(44), 444016 (2012).
138. K. Ding, Z. Zhang, and C. T. Chan, "Coalescence of exceptional points and phase diagrams for one-dimensional P T-symmetric photonic crystals," Phys. Rev. B **92**(23), 235310 (2015).
139. K. Ding, G. Ma, M. Xiao, Z. Zhang, and C. T. Chan, "Emergence, coalescence, and topological properties of multiple exceptional points and their experimental realization," Phys. Rev. X **6**(2), 021007 (2016).
140. B. Zhen, C. W. Hsu, Y. Igarashi, L. Lu, I. Kaminer, A. Pick, S. L. Chua, J. D. Joannopoulos, and M. Soljačić, "Spawning rings of exceptional points out of Dirac cones," Nature **525**(7569), 354–358 (2015).
141. M. Pan, H. Zhao, P. Miao, S. Longhi, and L. Feng, "Photonic zero mode in a non-Hermitian photonic lattice," Nat. Commun. **9**(1), 1308 (2018).
142. Y. Xu, S. T. Wang, and L. M. Duan, "Weyl Exceptional Rings in a Three-Dimensional Dissipative Cold Atomic Gas," Phys. Rev. Lett. **118**(4), 045701 (2017).
143. H. Shen, B. Zhen, and L. Fu, "Topological band theory for non-Hermitian Hamiltonians," Phys. Rev. Lett. **120**(14), 146402 (2018).
144. K. Kawabata, K. Shiozaki, and M. Ueda, "Non-Hermitian Chern insulator," arXiv preprint arXiv:1805.09632 (2018).
145. S. Yao, F. Song, and Z. Wang, "Non-Hermitian Chern bands and Chern numbers," arXiv preprint arXiv:1804.04672 (2018).
146. V. Alvarez, J. Vargas, M. Berdakin, and L. Torres, "Topological states of non-Hermitian systems," arXiv preprint arXiv:1805.08200 (2018).
147. S. Yao and Z. Wang, "Edge states and topological invariants of non-Hermitian systems," arXiv preprint arXiv:1803.01876 (2018).
148. T. Bar, S. K. Choudhary, M. A. Ashraf, K. S. Sujith, S. Puri, S. Raj, and B. Bansal, "Kinetic Spinodal Instabilities in the Mott Transition in V_{2}O_{3}: Evidence from Hysteresis Scaling and Dissipative Phase Ordering," Phys. Rev. Lett. **121**(4), 045701 (2018).
149. T. Bar, S. K. Choudhary, M. A. Ashraf, K. S. Sujith, S. Puri, S. Raj, and B. Bansal, "Kinetic spinodal instabilities in the Mott transition in V_{2}O_{3}: Evidence from hysteresis scaling and dissipative phase ordering," Phys. Rev. Lett. **121**(4), 045701 (2018).
150. H. Zhou, C. Peng, Y. Yoon, C. W. Hsu, K. A. Nelson, L. Fu, J. D. Joannopoulos, M. Soljačić, and B. Zhen, "Observation of bulk Fermi arc and polarization half charge from paired exceptional points," Science **11**, 9859 (2018).
151. E. Khalaf, "Higher-order topological insulators and superconductors protected by inversion symmetry," Phys. Rev. B **97**(20), 205136 (2018).
152. F. Schindler, A. M. Cook, M. G. Vergniory, Z. Wang, S. S. Parkin, B. A. Bernevig, and T. Neupert, "Higher-order topological insulators," Phys. Rev. B **97**(20), 205136 (2018).
153. M. Geier, L. Trifunovic, M. Hoskam, and P. W. Brouwer, "Second-order topological insulators and superconductors with an order-two crystalline symmetry," Phys. Rev. B **97**(20), 205135 (2018).
154. W. A. Benalcazar, B. A. Bernevig, and T. L. Hughes, "Quantized electric multipole insulators," Science **357**(6346), 61–66 (2017).
155. W. A. Benalcazar, B. A. Bernevig, and T. L. Hughes, "Electric multipole moments, topological multipole moment pumping, and chiral hinge states in crystalline insulators," Phys. Rev. B **96**(24), 245115 (2017).

Optics EXPRESS

156. C. W. Peterson, W. A. Benalcazar, T. L. Hughes, and G. Bahl, "A quantized microwave quadrupole insulator with topologically protected corner states," Nature **555**(7696), 346–350 (2018).
157. B. Y. Xie, H. F. Wang, H. X. Wang, X. Y. Zhu, J. H. Jiang, M. H. Lu, and Y. F. Chen, "Second-order topological photonic insulator with corner states," arXiv preprint arXiv:1805.07555v2 (2018).
158. M. Ezawa, "Topological switch between second-order topological insulators and topological crystalline insulators," arXiv preprint arXiv:1806.03007 (2018).
159. J. Noh, W. A. Benalcazar, S. Huang, M. J. Collins, K. P. Chen, T. L. Hughes, and M. C. Rechtsman, "Topological protection of photonic mid-gap defect modes," Nat. Photon., **12**(**7**) 408-415 (2018).
160. L. Esposito and D. Gerace, "Topological aspects in the photonic-crystal analog of single-particle transport in quantum Hall systems," Phys. Rev. A **88**(1), 013853 (2013).
161. R. Sepkhanov, J. Nilsson, and C. Beenakker, "Proposed method for detection of the pseudospin-1 2 Berry phase in a photonic crystal with a Dirac spectrum," Phys. Rev. B **78**(4), 045122 (2008).
162. Q. Wang, M. Xiao, H. Liu, S. Zhu, and C. T. Chan, "Measurement of the Zak phase of photonic bands through the interface states of a metasurface/photonic crystal," Phys. Rev. B **93**(4), 041415 (2016).
163. M. Xiao, G. Ma, Z. Yang, P. Sheng, Z. Zhang, and C. T. Chan, "Geometric phase and band inversion in periodic acoustic systems," Nat. Phys. **11**(3), 240–244 (2015).
164. L. Duca, T. Li, M. Reitter, I. Bloch, M. Schleier-Smith, and U. Schneider, "An Aharonov-Bohm interferometer for determining Bloch band topology," Science **347**(6219), 288–292 (2015).
165. M. Hafezi, "Measuring topological invariants in photonic systems," Phys. Rev. Lett. **112**(21), 210405 (2014).
166. M. Atiyah, *K-theory* (CRC Press, 2018).
167. E. Witten, "Topological quantum field theory," Commun. Math. Phys. **117**(3), 353–386 (1988).
168. X. Chen, Z. C. Gu, Z. X. Liu, and X. G. Wen, "Symmetry-protected topological orders in interacting bosonic systems," Science **338**(6114), 1604–1606 (2012).
169. R. W. Boyd, "Nonlinear optics, 3rd," (Academic press, 2008).
170. M. Hafezi, P. Adhikari, and J. M. Taylor, "Engineering three-body interaction and Pfaffian states in circuit QED systems," Phys. Rev. B **90**(6), 060503 (2014).
171. H. Schomerus and N. Y. Halpern, "Parity anomaly and Landau-level lasing in strained photonic honeycomb lattices," Phys. Rev. Lett. **110**(1), 013903 (2013).
172. G. Salerno, T. Ozawa, H. M. Price, and I. Carusotto, "Propagating edge states in strained honeycomb lattices," Phys. Rev. B **95**(24), 245418 (2017).
173. F. de Juan, M. Sturla, and M. A. Vozmediano, "Space dependent Fermi velocity in strained graphene," Phys. Rev. Lett. **108**(22), 227205 (2012).
174. G. Salerno, T. Ozawa, H. M. Price, and I. Carusotto, "How to directly observe Landau levels in driven-dissipative strained honeycomb lattices," 2D Materials **2**(3), 034015 (2015).
175. M. C. Rechtsman, J. M. Zeuner, A. Tünnermann, S. Nolte, M. Segev, and A. Szameit, "Strain-induced pseudomagnetic field and photonic Landau levels in dielectric structures," Nat. Photonics **7**(2), 153–158 (2013).
176. F. Zhong, J. Li, H. Liu, and S. Zhu, "Controlling surface plasmons through covariant transformation of the spin-dependent geometric phase between curved metamaterials," Phys. Rev. Lett. **120**(24), 243901 (2018).

1. Introduction

As argued by P. W. Anderson in 1972 [1], nature is not in the way that can be understood by reductionism: that the cognition of a system can be understood by studying its individual, constituent parts and their interactions. Although it is primarily discussed in the field of condensed matter physics, this argument may find a support when we study the photonic crystals. While the basic physical laws describing electromagnetic (EM) waves are the Maxwell equations, understanding the physical properties of EM waves in photonic crystals needs a whole new conceptual structure which can be borrowed from condensed matter physics and topology.

Photonic crystal (PC) branches from the idea to control the optical properties of materials in a similar way to control the electrical properties in condensed matter physics [2]. It was first proposed in 1987 by E. Yablonovitch [3] and S. John [4] that, by periodically arranging macroscopic materials with different dielectric constants (or functions) in space, the propagations of EM waves will be dramatically changed due to the refractions and reflections. Particularly, there is a kind of PCs that possess photonic band gap (PBG) suppressing the propagation of EM waves with certain frequencies [2]. In past few decades, tremendous studies of PCs consisting of all-dielectric materials [2], optical resonators [5] and metamaterials [6] with different lattice structures indicated the existence of various band properties which can be used to design novel optical devices. For a long time, the studies of PCs are focused on the local band structures with unique optical properties and their applications such as designing a mirror, a waveguide, and a cavity.

Optics EXPRESS

Recently, as the topological phases of matters have been discovered in electronic materials [7–9], the exploration of band properties in PCs meets a new inflexion where the overall topological properties have been focused. The topological phases of matters have unique effects which cannot be explained by the spontaneous symmetry-breaking mechanism such as the integer quantum Hall effect (IQHE) [10], quantum anomalous Hall effect (QASE) [11] and quantum spin Hall effect (QSHE) [12]. However, all of these topological phases can be well described by the topological band theory [9]. The topological band theory is primarily developed for describing the topological properties of single-particle Hermitian systems. The simplest case is the IQHE in 2-dimensional (2D) electron gas with a uniform external magnetic field applied in the vertical direction [10]. The energies of circular moving electrons are quantized to form the Landau levels which can be regarded as the band structures if we define an area with flux quantum as the lattice plaquette. In this case, the band structures are many flat bands independent of crystal momentum **k** while in real crystals the bands disperse with **k**. The topological protected quantized Hall conductivity is characterized by a non-trivial topological invariant which is the same as the non-trivial Chern number (or TKNN number) [13]. Since the translational symmetry always exists in crystals, the crystal momentum **k** is well defined. The band structures are calculated from the equation $\mathcal{H}(\mathbf{k})\left|u_n(\mathbf{k})\right\rangle = E_n(\mathbf{k})\left|u_n(\mathbf{k})\right\rangle$ where $\mathcal{H}(\mathbf{k})$, $\left|u_n(\mathbf{k})\right\rangle$ and $E_n(\mathbf{k})$ is the Bloch Hamiltonian, Bloch wavefunction and eigenvalue for the nth band respectively. As **k** goes around the Brillouin zone (BZ), the Bloch wave function acquires a geometric phase which is the Berry phase. The Chern number of the nth band is defined as the Berry phase accumulation when **k** goes around the whole BZ:

$$C_n = \frac{1}{2\pi}\int_{BZ} \mathrm{d}^2\mathbf{k}\mathcal{F}_n \tag{1}$$

where $\mathcal{F}_n = \nabla \times \mathcal{A}_n$ is the Berry curvature and $\mathcal{A}_n = i\left\langle u_n\right|\nabla_{\mathbf{k}}\left|u_n\right\rangle$ is the Berry connection. The total Chern number is defined as the summation of the Chern numbers of all occupied bands $C = \sum_{n=1}^{N} C_n$ and does not change provided that the band gap separating occupied bands and empty bands remains finite. For the trivial insulating phase, the total Chern number equals to zero while for the non-trivial insulating phase, it equals to a non-zero integer.

The emergence of topological phases in electronic materials is related to the wave-particle duality of electrons. This perception stimulates the exploration of topological phases in classic wave systems. In fact, in many systems with periodically modulated waves such as the PCs, phononic crystals [14], surface plasmons [15] and mechanic systems [16], the topological phases can emerge as the manifestation of geometric properties.

In this Review, starting from the classification of topological phases with respect to symmetries, we give a presentation about topologically gapped phases as well as topologically gapless phases in photonics. Other topological phases in photonics such as topological non-Hermitian photonic systems, higher-order topological phases and geometric phases in photonic systems have been discussed. Finally, we conclude by providing the outlooks for future studies of topological phases in photonics.

2. Topologically gapped phases in photonic crystals

A unique character of topological gapped phases is that there is gapless edge state emerging at the interface between two topologically gapped phases within different topological classes [7, 8]. An easy but not rigorous way to understand this fact is that since nature has no mutation, if we go from a gapped phase to another gapped phase, at the interface, the gap must be closed and hence the gapless state emerges. Additionally, the edge state is robust against disorders and perturbations as long as the topological classes of both sides do not change.

Optics EXPRESS

2.1. Topological classification of gapped systems

For the gapped systems, the Hamiltonians can be classified into topological equivalent classes in which the Hamiltonians can be adiabatically deformed into each other without closing the bandgaps [14]. The discrete symmetries play an important role in determining the band structures and therefore it is possible to topologically classify the gapped systems with respect to different discrete symmetries such as the time-reversal symmetry (T), particle-hole symmetry (C) and chiral symmetry (S). These three symmetries act on the single-particle Hamiltonian as:

$$\begin{aligned} TH(\mathbf{k})T^{-1} &= H(-\mathbf{k}) \\ CH(\mathbf{k})C^{-1} &= -H(-\mathbf{k}) \\ SH(\mathbf{k})S^{-1} &= -H(\mathbf{k}) \end{aligned} \tag{2}$$

In terms of the first quantization of the system where electrons are described by the wavefunctions and the energies of them are discretized, if the Hamiltonian is regularized on a finite lattice, we can represent the Hamiltonian by using a $N \times N$ matrix. Clearly, the discrete symmetries put constraints on the regularized Hamiltonian and determine the type of matrix that the quantum mechanical time-evolution operator $\exp(\mathrm{i}tH)$ in. For a concrete example, if T = 0, S = 0, and C = 0, there is no constrains and $\exp(\mathrm{i}tH)$ is an element of the unitary group $U(N)$ which is regarded as the symmetric space of the matrix. Classified by Cartan in 1926, in terms of these three symmetries, there are totally ten symmetric spaces which correspond to ten classes as listed in Table 1. Next, considering the non-linear sigma model (NLσM) for random systems which describes the boundary topological properties of gapped systems in ten symmetric classes, the topological classes and topological invariants can be determined by studying the homotopy groups for each target spaces of NLσM. The classification is shown in Table 1 which is regarded as the periodic table for topologically gapped phases [17, 18].

Classifications of topological gapped phases with respect to other discrete symmetries such as the reflection symmetry [17, 19, 20], point group symmetry [21], space group symmetry [22], order-two spatial symmetry [23] Floquet-Bloch system [24, 25] and non-symmorphic symmetry [26] show the strong relation between discrete symmetries and topological properties of systems which provides instructions to experimental designations of system with certain topological gapped phases and boundary states

2.2. Topological gapped photonic crystals without T symmetry

The first theoretical prediction of topological gapped phase in photonic crystal (PC) which is described by a Hermitian single-particle effective Hamiltonian is given by Haldane and Raghu [27] in gyromagnetic 2D hexagonal PC. The master equation of PC is:

$$\nabla \times [\overleftrightarrow{\mu}^{-1}(\mathbf{r}) \nabla \times \mathbf{E}] = \overleftrightarrow{\epsilon}(\mathbf{r}) \omega^2 \mathbf{E} \tag{3}$$

where $\overleftrightarrow{\mu}$ and $\overleftrightarrow{\epsilon}$ are permeability tensors and permittivity tensor respectively. ω and $\mathbf{E}$ are the eigenfrequency and corresponding electric field. They proposed a photonic analog of IQHE in 2D PC slab. From the perspective of topological band theory, they defined the photonic Berry connection of the bands:

Optics EXPRESS

Table 1. - Classification of topological insulators and topological superconductors with respect to time-reversal symmetry (T), particle-hole symmetry (C) and chiral symmetry (S). Number 0 (1) for S means no (have) chiral symmetry. Since time-reversal operator and particle-hole operators are anti-unitary operators and square to ± 1, there are three types: even, odd and absent which are represented by + 1, –1 and 0 respectively. d represents the spatial dimension of the system. The notation of ten classes follows the notation invented by Cartan, Altland and Zirnbauer (CAZ) [28, 29]. The entries 0, $\mathbb{Z}$, $\mathbb{Z}_2$ and $2\mathbb{Z}$ represents the topological invariants of each Hamiltonians which correspond to 0, an integer, an integer of mod 2 and an even integer respectively. Table. 1 is reproduced with permission from [18]. Copyright 2010, IOP Publishing.

	Symmetry			*d*							
Class	T	C	S	0	1	2	3	4	5	6	7
A	0	0	0	$\mathbb{Z}$	0	$\mathbb{Z}$	0	$\mathbb{Z}$	0	$\mathbb{Z}$	0
AIII	0	0	1	0	$\mathbb{Z}$	0	$\mathbb{Z}$	0	$\mathbb{Z}$	0	$\mathbb{Z}$
AI	+1	0	0	$\mathbb{Z}$	0	0	0	$2\mathbb{Z}$	0	$\mathbb{Z}_2$	$\mathbb{Z}_2$
BDI	+1	+1	1	$\mathbb{Z}_2$	$\mathbb{Z}$	0	0	0	$2\mathbb{Z}$	0	$\mathbb{Z}_2$
D	0	+1	0	$\mathbb{Z}_2$	$\mathbb{Z}_2$	$\mathbb{Z}$	0	0	0	$2\mathbb{Z}$	0
DIII	-1	+1	1	0	$\mathbb{Z}_2$	$\mathbb{Z}_2$	$\mathbb{Z}$	0	0	0	$2\mathbb{Z}$
AII	-1	0	0	$2\mathbb{Z}$	0	$\mathbb{Z}_2$	$\mathbb{Z}_2$	$\mathbb{Z}$	0	0	0
CII	-1	-1	1	0	$2\mathbb{Z}$	0	$\mathbb{Z}_2$	$\mathbb{Z}_2$	$\mathbb{Z}$	0	0
C	0	-1	0	0	0	$2\mathbb{Z}$	0	$\mathbb{Z}_2$	$\mathbb{Z}_2$	$\mathbb{Z}$	0
CI	+1	-1	1	0	0	0	$2\mathbb{Z}$	0	$\mathbb{Z}_2$	$\mathbb{Z}_2$	$\mathbb{Z}$

$$\mathbf{A}^{nn'}(\mathbf{k}) = i\left\langle \mathbf{E}_{n\mathbf{k}} \middle| \nabla_{\mathbf{k}} \middle| \mathbf{E}_{n'\mathbf{k}} \right\rangle \tag{4}$$

where $\mathbf{E}_{n\mathbf{k}}$ is the periodic part of the electric-field Bloch function. The corresponding Chern number for the photonic band is:

$$C_n = \frac{1}{2\pi i}\int_{BZ} \mathrm{d}^2\mathbf{k}\left(\frac{\partial A_y^{nn}}{\partial k_x} - \frac{\partial A_x^{nn}}{\partial k_y}\right) \tag{5}$$

where the BZ stands for the first Brillouin zone. To introduce topologically non-trivial pairs of Chern numbers near the degenerate points, they considered hexagonal lattice geometry where there are Dirac points in the Brillouin zone corners when both T and parity (P) symmetries are kept. If T and P are broken, the Dirac point degeneracy is lifted and the band structure of PC becomes gapped. However, if P is broken alone and the PC have only T symmetry, the Berry curvature:

$$\mathcal{F}_{xy}(\mathbf{k}) = \frac{\partial A_y^{nn}}{\partial k_x} - \frac{\partial A_x^{nn}}{\partial k_y} \tag{6}$$

is an odd function of **k** and the thus the Chern number equals to zero. In contrary, if T is broken alone and P is reserved, $\mathcal{F}_{xy}(\mathbf{k})$ is an even function of **k** and the Chern number is nonzero. To achieve topological non-trivial gapped phase in PC, considering the magneto-optical effect which breaks T but keeps P:

Optics EXPRESS

$$\overleftrightarrow{\mu} = \begin{bmatrix} \mu & i\kappa & 0 \\ -i\kappa & \mu & 0 \\ 0 & 0 & \mu_0 \end{bmatrix} \tag{7}$$

the non-zero Chern number and corresponding unidirectional edge states emerge. Direct calculation of total Chern number shows that it is an integer.

From the perspective of topological classification, since T = 0, C = 0, and S = 0, the target space of NLσM is $U(2n)/[U(n)\times U(n)]$ as shown in [18]. Moreover, since the spatial dimensionality d = 2, the homotopy group is $\pi_2(U(2n)/[U(n)\times U(n)]) = \mathbb{Z}$. Therefore, the PC is in class A and characterized by $\mathbb{Z}$ type topological invariant which is the integer Chern number. The edge states are robust against elastic backscattering due to the topological protection of the bulk band gap.

The first theoretical [30] and experimental realization [31] of this gapped photonic phase is proposed by Wang et al. in gyromagnetic PC. The experimental setup is shown in Fig. 1(a)-(b). The 2D PC slab consists of gyromagnetic ferrite rods in the air with a square lattice structure. To forbid the radiation of EM wave to the air, the PC is covered by copper for confinement. The unidirectional edge states are measured by the transmission spectra in the forward direction and backward direction as shown in Fig. 1(e). Figure 1(c)-(d) present the numerical simulation results.

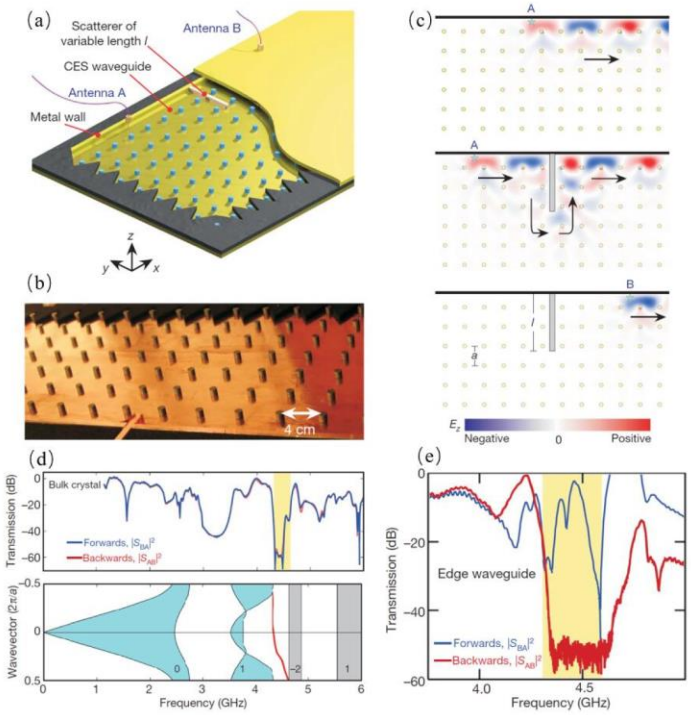

Fig. 1. The experimental setup and numerical simulation results. (a). The layout of the PC consisted of gyromagnetic rods which are confined by metal walls. (b). The photograph of the PC with the top plate removed. (c). Numerical simulation shows that there is a unidirectional edge state propagating along the interface without backscattering which is robust against an obstacle. (d). The transmission spectra of the PC without confinement and the projected PC band structure. There is a clear suppress of transmission at the frequencies in the PBG. The red line represents the gapless edge state. (e). Transmission spectra of the confined PC where the spectra are non-reciprocal which shows the edge states propagate unidirectionally at the interface. (a)-(e) are reprinted with permission from [31]. Copyright 2009, Springer Nature.

Optics EXPRESS

The T-symmetry breaking topological gapped phases and their unique edge states in gyromagnetic PC have been extensively studied by others. For example, it was shown that the gapped phases and gapless edge states can emerge in PC without confinement where the dispersions of the gapless edge states are below the light line [32–34]. Besides, if several Dirac cone degeneracies simultaneously lifted, gapped phases with larger Chern number can be realized as shown in [35, 36] which can be easily understood as adding several copies of previous systems together in 2D. Another interesting phenomenon is that the topological gapped phase and robust edge states can exist even in amorphous systems [37, 38] which shows the topological characters of this phase. Similar studies [39–44] have discussed the realizations of T symmetry breaking phases in gyromagnetic PC. In terms of application, the T-symmetry breaking topological gapped phases have been proposed for designing novel optical devices [45–54].

In addition to the gyromagnetic materials, it is feasible to realize T-symmetry breaking topological gapped phases in other systems. As an example, it is proposed that, in optomechanical resonators where photons interact with phonons confined in a cavity, if we choose one circulation direction by using directional laser pumping, the T-symmetry breaking topological gapped phase emerges as a consequence of non-reciprocal transport of photons [55].

2.3. Topological gapped photonic crystals with T symmetry

Previous studies of topological T-symmetry breaking gapped PC require magneto-optical effect which is limited to the microwave frequencies and becomes very weak in the optical domain [56]. To achieve topological gapped phases with robust edge states in optical frequencies, one possible approach is to find the photonic analog of QSHE where T symmetry is kept [12]. Comparing to T-symmetry breaking IQHE, QSHE in electric materials has two counter propagating edge states with different spin polarization in each propagating direction. Therefore, the net electric current and corresponding Chern number equal to zero while the net-spin current and corresponding spin Chern number are non-zero.

However, comparing to electrons which are spin $1/2$ fermions, the photons are spin-1 bosons and have no counterparts of two degenerate modes in the spin degree of freedom. One way to solve this problem is to introduce a pseudo-spin degree of freedom and pseudo-T symmetry with $T^2 = -1$ in PC which means that there are two degenerate modes connected by pseudo-T symmetry and can be regarded as spin degeneracy [57–59]. Imagining that there are two copies of modes in PC where there is no mixing between them, for each copy, there is a non-zero Chern number (spin Chern number) defined on that species. Moreover, since two modes are propagating in opposite directions, the spin Chern numbers of two species have opposite sign and thus the total Chern number vanishes. Nevertheless, we can define a non-zero topological invariant for the PC by considering the subtraction rather than the summation of two spin Chern numbers.

The first theoretical proposal [60] of QSHE in photonics utilized coupled resonator optical waveguide (CROW) arrayed in a 2D square lattice as shown in Fig. 2(c). The degenerate pseudo-spin up and pseudo-spin down states are represented by degenerate whispering-gallery modes which propagate clockwise and counter-clockwise in CROW respectively as shown in Fig. 2(a). Furthermore, if there are no scatterers in resonators and waveguides, these two species of pseudo-spins propagating in opposite directions do not mix with each other which is similar to the spin-momentum locking in QSHE. The evanescent couplings between resonators lead to a tight-bind model for charged bosons with a synthetic magnetic field for photons in the perpendicular direction. For the system in Fig. 2(c), the tight-binding Hamiltonian is given by [60]:

$$H_0 = -\kappa\Big(\sum_{\sigma,x,y} \hat{a}^{\dagger}_{\sigma x+1,y}\hat{a}_{\sigma x,y}e^{-i2\pi\alpha y\sigma} + \hat{a}^{\dagger}_{\sigma x,y}\hat{a}_{\sigma x+1,y}e^{i2\pi\alpha y\sigma} + \hat{a}^{\dagger}_{\sigma x,y+1}\hat{a}_{\sigma x,y} + \hat{a}^{\dagger}_{\sigma x,y}\hat{a}_{\sigma x,y+1}\Big) \quad (8)$$

Optics EXPRESS

Here κ is the coupling rate of optical modes and $\hat{a}^{\dagger}_{\sigma x,y}$ ($\hat{a}_{\sigma x,y}$) is the photon creation (annihilation) operator at lattice site (x, y) with pseudo-spin components, $\sigma = \pm 1$. Consequently, the photonic band structure can be calculated by solving the tight-binding Hamiltonian as shown in Fig. 2(e). The T-symmetry preserving topological gapped phases are

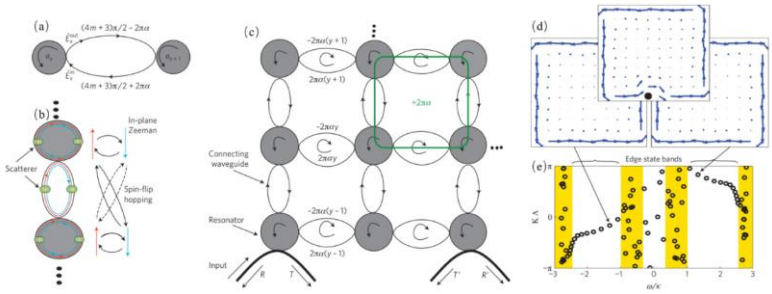

Fig. 2. QSHE in CROW. (a). Two coupled resonators with different lengths of the upper and lower branches. (b). If we introduce scatterers in resonators and waveguides, we can achieve in-plane magnetic field and spin-flip hopping terms. (c). 2D CROW which can be described by a tight-binding model. (d). Demonstration of forward- and backward-propagating edge states with different pseudo-spin components. The edge states are robust against disorders. (e). Projected band structure of CROW which shows two edge states in the band gaps. (a)-(e) are reprinted with permission from [60]. Copyright 2013, Springer Nature.

characterized by the spin Chern number defined in the bulk bands and the topologically protected edge states appear which is robust against disorders as shown in Fig. 2(d). If we include semi-transparent scatterers inside the resonators and waveguides, two pseudo-spin components are coupled and we can achieve pseudo-spin-orbital interaction in CROW as shown in Fig. 2(b). The above system was realized in experiment [61] by using standard silicon-on-insulator technology which can be used to design optical robust delay lines.

The edge states at the interface of two quantum spin Hall (QSH) topological gapped systems have some different features from the edge states in quantum Hall systems. First, the edge states are reciprocal which means that light can propagate either forward or backward. Second, from the viewpoint of classification Table [18], since T = –1, C = 0, and S = 0, the target space of NLσM is $O(2n)/[O(n)\times O(n)]$ as shown in [18]. Moreover, since the spatial dimensionality d = 2, the homotopy group is $\pi_2(O(2n)/[O(n)\times O(n)]) = \mathbb{Z}_2$. the system is in AII class and characterized by a $\mathbb{Z}_2$ topological invariant. The robustness of edge states against sharp bending, random distribution of synthetic gauge field, lattice disorder has been experimentally verified.

So far, we have reviewed the QSHE in CROW. Nevertheless, it is feasible to realize QSHE in other optical systems. For example, in free space, the light exhibits an intrinsic QSHE where there are evanescent surface modes with strong spin-momentum locking [62, 63]. Here the spin components are represented by left- and right-handed circular polarizations of light which have opposite helicities. The spin vector is locked to the propagation vector. However, since it is an intrinsic property of EM wave, there is no pseudo-T symmetry with $T^2 = -1$ and the real T symmetry for bosonic waves squares to + 1. Therefore, the corresponding edge states are not topologically protected by T symmetry and not free from backscattering. Nevertheless, this system provides robust unidirectional spin transport.

Additionally, as proposed by Khanikaev et al. [64], QSHE can be realized in bianisotropic metamaterials. In this case, the spin components are represented by two linear combinations of transverse electric (TE) and transverse magnetic (TM) modes. These spins states are connected by a pseudo-T symmetry with $T^2 = -1$. Comparing to CROW, the bianisotropic metamaterials can be fabricated at the size which is in the same order of EM wavelength and therefore have an advantage in footprint [58]. The spin-polarized edge states are robust

Optics EXPRESS

against disorders and free from backscattering. Another advantage of using metamaterials to realize T-symmetric topological gapped phases is that it is possible to achieve reconfigurable topological phases as pointed by [65–68] where the PC consists of meta-waveguides with adjustable structures. By moving the metallic rods at different positions, the PC goes from symmetric (no bianisotropic with gapless Dirac cone) to asymmetric (bianisotropic with Dirac cone opened) structures [66]. The reduction of symmetry induces a mixing of the four original Dirac bands-the lower antisymmetric (symmetric) mode and upper symmetric (antisymmetric) mode to form two pseudo-spins with spin-momentum locked. Recently, this work has been generalized to all-dielectric bianisotropic metamaterials where the losses are reduced and could be realized at optical frequencies [69].

One of the key steps of realizing QSHE in PC is to construct pseudo-spins and corresponding T symmetry. Comparing to previous platforms with dedicated structures which may be difficult to realize in applications, recently, Wu and Hu [70] have theoretically proposed and experimentally realized [71] an all-dielectric material in which QSHE can be

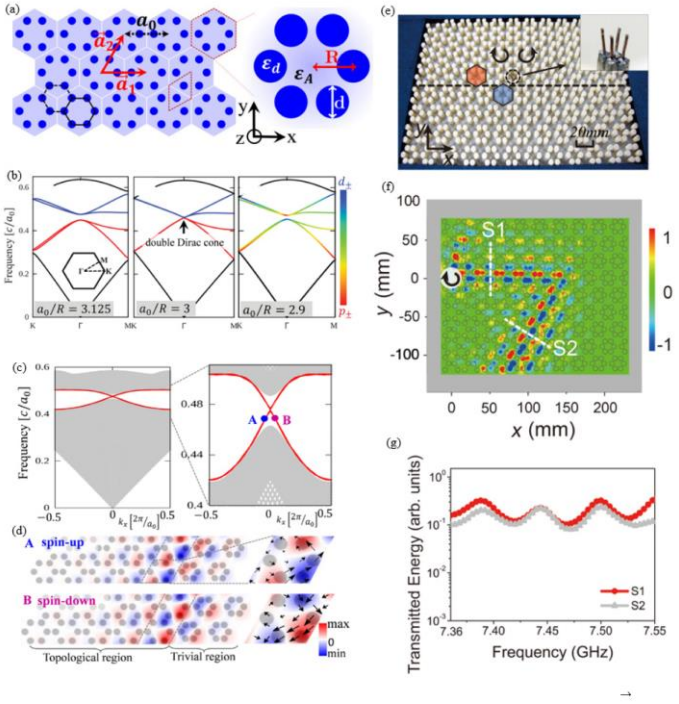

Fig. 3. QSHE in all-dielectric PCs. (a). Schematic plot of PC with the lattice vectors a_1 and $\vec{a}_2$, the lattice constant a_0, the dielectric constants of rods and background ε_d and ε_A, the diameter of rods d. (b). Band inversion process induced by reducing the lattice constant from extended phase to shrunk phase. (c). Numerical calculation of the projected band structures shows that there are two topological edge states with opposite group velocities emerging at the band gap. (d). Real space distribution of the E_z field at point A and B indicated in (c). Two pseudo-spin components propagate along opposite directions. (e). Experimental setup of PC with extended and shrunk configurations. A square-shaped antenna array is used to selectively excite certain EM pseudo-spin state indicated by circular arrows. (f). Clockwise pseudo-spin state is excited and propagates along the interface of two topologically inequivalent configurations where the edge states are robust against sharp corners. (g). Transmission measured at two different positions indicated in (f) which shows that there is no backscattering of the edge states. (a)-(d) are reprinted with permission from [70]. Copyright 2015, American Physical Society. (e)-(g) are reprinted with permission from [71]. Copyright 2018, American Physical Society.

Optics EXPRESS

induced by deforming a honeycomb lattice of rods into triangular lattice of rod hexagons as shown in Fig. 3(a) and (e). As is known, at the Brillouin zone corners of honeycomb lattice K and K', there are two-fold degenerate points which form the Dirac cone structures [27]. However, if we regard the honeycomb lattice as a triangular lattice of hexagonal clusters composed by six neighboring sites, the two Dirac cone structures at Brillouin zone corner will be moved to the Brillouin center Γ point and form doubly degenerate Dirac cones as shown in Fig. 3(b). Then the doubly degenerate Dirac cones are opened by extending or shrinking the clusters while keeping the C_{6v} symmetry of the hexagonal clusters. the TM modes hosted by the clusters which are regarded as "artificial atoms" exhibit electronic orbital-like p- and d-wave shapes. For the upper bands, there are p_x and p_y photonic orbitals while for the lower bands, there are d_{xy} and $d_{x^2-y^2}$ photonic orbitals [70, 72]. With respect to the inversion symmetry, these four states can be linearly combined into symmetric and asymmetric form $p_\pm=(p_x \pm ip_y)/\sqrt{2}$ and $d_\pm=(d_{x^2-y^2} \pm id_{xy})/\sqrt{2}$ which are two pseudo-spin components. A band inversion takes place as we reduce the lattice constant from extended phase to a shrunk phase which results in non-trivial $\mathbb{Z}_2$ topology and topologically protected edge states as shown in Fig. 3(c)-(g).

Essentially, this approach is the same as the quantum valley Hall effect (QVHE) [73, 74]. The valley degree of freedom arises from the C_{6v} point group symmetry where the PC has two inequivalent Brillouin zone corners. It has been extensively studied in condensed matter physics for the potential application in valleytronics [75, 76]. If the photons cannot be scattered from one valley to another, the valley is a good degree of freedom which can be used to realize T-symmetric topologically gapped phases in PCs [77, 78]. An interesting case is that when the PC has both spin and valley degree of freedoms, then it is possible to design exotic spin-valley-polarized photonic states [79, 80].

The realization of QSHE and QVHE in photonics with T symmetry and topologically protected edge states has been extended to other systems such as the topological RF circuits [81], twisted optical resonators [82] which have been well reviewed in [57].

2.4 Crystalline symmetries protected topological gapped phases in PC

2.4.1 Topological gapped PC with point group symmetries

Other than aforementioned T and P symmetries, point group symmetries can also lead to non-trivial topologically gapped phases [83]. For example, the topological crystalline insulators have been theoretically proposed [84] where there are topological metallic surface states with quadratic band degeneracy on high symmetric crystal surfaces which are protected by C_4 point group symmetry without spin-orbital coupling. The bulk bands and edge states are characterized by new topological invariants.

Recently the studies of 2D PC in square lattice [85, 86] indicated that there are topological gapped phases as well as gapless edge states in both electronic materials and PCs which are protected by C_4 point group symmetry. Moreover, the topological non-trivial PBG and robust edge states are characterized by 2D Zak phase with zero Berry curvature.

2.4.2 Topological gapped PC with non-symmorphic group symmetry

In addition to point group symmetry, there is another subset of space group symmetry which is the non-symmorphic group symmetry. The non-symmorphic group symmetry operation is a combination of a point group symmetry operation and a nonprimitive lattice transformation. A couple of recent studies about non-symmorphic symmetry in electronic materials have revealed the existence of topologically non-trivial gapped phases [87–90]. For the topologically gapped phases, a non-symmorphic crystalline insulator with $\mathbb{Z}_2$ topology has been proposed which supports gapless boundary states with Mobius twisted energy dispersion

Optics EXPRESS

[90]. The non-symmorphic group symmetry protected topologically gapped phases do not require T symmetry and is not limited to fermionic systems. Therefore, it can appear in bosonic systems such as PCs.

2.5 Floquet topological photonic gapped phases

Previous studies of topologically non-trivial phases are all about static systems. When time-dependent modulations are considered, new topological gapped phases emerge as the manifestation of non-equilibrium topological states. Moreover, the spectral properties such as the velocity of edge states, the bandgap of the bulk insulators can be directly controlled. Unlike the electronic materials where the time-dependent modulation is introduced by irradiation with microwave frequencies [91], in PCs, periodic modulation of the z-direction is regarded as time modulation. This kind of PCs with non-trivial topologically gapped phases are called photonic Floquet topological insulators (PFTI). The first experimental realization of PFTI achieved by Rechtsman et al. [92] They consider a 2D hexagonal photonic waveguide array periodically modulated in the z-direction as shown in Fig. 4(a)-(b). The waveguides are fabricated by using the femtosecond laser writing method. In analogy to Floquet topological insulator, the Maxwell equation which describes the paraxial propagation of light in this PC is transformed into the Schrödinger-type equation [92]:

$$i\partial_z \psi(x,y,z) = -\frac{1}{2k_0}\nabla^2\psi(x,y,z) - \frac{k_0\Delta n(x,y,z)}{n_0}\psi(x,y,z) \tag{9}$$

where $\psi(x,y,z)$ is defined as $\mathbf{E}(x,y,z) = \psi(x,y,z)\exp(ik_0 z - i\omega t)\mathbf{x}$. $\mathbf{E}$, x, t, k_0 stand for electric field, unit vector, time, wavenumber in the ambient medium. $\Delta n(x,y,z)$ is the effective potential. As the waveguides twist in the z-direction, the synthetic magnetic field appears and Floquet states with robust edge states emerge as shown in Fig. 4(c)-(d). Interestingly, the transverse group velocity of the edge state is relevant to the helix radius as shown in Fig. 4(e).

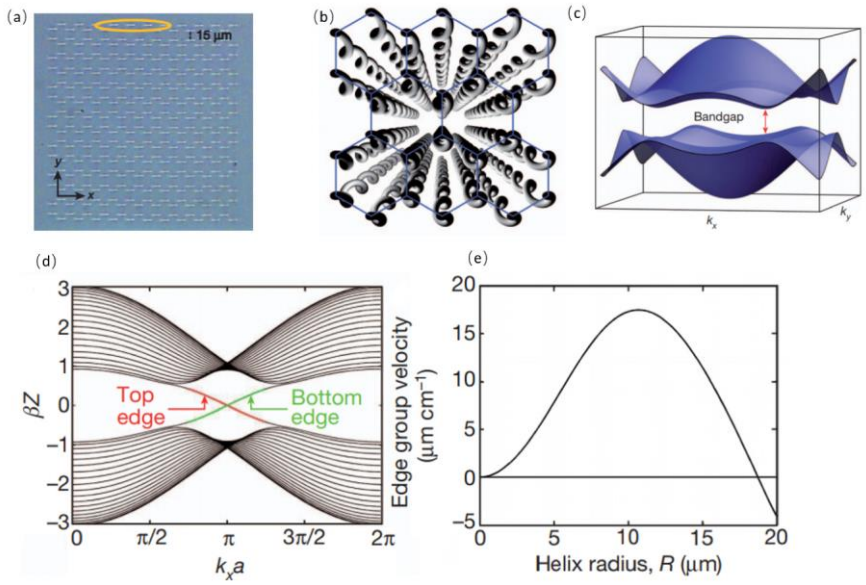

Fig. 4. Floquet topological gapped phases in PCs. (a). Image of the PC at the input facet. (b). Schematic of the helical waveguides. (c). Band structure of the PC when rotation radius is not zero where there is a bandgap. (d). Projected band structure of (c). There are two edge states with non-zero group velocity. (e). The group velocity of edge states is relevant to the radius of rotation. (a)-(e) are reprinted with permission from [92]. Copyright 2013, Springer Nature.

Optics EXPRESS

The Floquet topological edge states are topologically robust against sharp corner and defect. In this example, fast-rotating modulation is considered in order to avoid coupling between different Flouquet orders. Recently, the hybridization of bands in different Floquet orders which non-trivial topology has been considered to form the anomalous Floquet topological insulator [25, 93, 94].

3. Topological gapless photonic crystals

3.1 Topological classification of gapless systems

The topological properties of band structure not only manifest itself on bandgaps in which there may be topologically protected edge states but also involve the band degeneracies which is regarded as gapless structures such as the gapless points, gapless nodal lines and gapless surfaces [95]. In terms of topology, the gapless structures are topologically stable in momentum space against disorders. For example, they can be moved or deformed but cannot disappear provided that there is no topological phase transition. In momentum space, the gapless structures can be regarded as magnetic singularities which determine the distribution of Berry curvature [96]. Similar to real space singularities of the electric field, for each gapless structure, a topological charge can be allocated to it which characterized the topological properties. Topological classification of gapless structures in momentum space for Hermitian single-particle systems has been done in [95]. We define the codimension of a gapless structure as $p = d - d_F - 1$ where d_F is the dimension of gapless structure, d is the spatial dimension of the system. Considering time-reversal, particle-hole and chiral symmetries, the gapless structures can be classified into ten classes with respect to different codimenions as shown in Table 2. The similarity between the classification table of gapless structures and the one of gapped phases has been revealed in [97].

Table 2. Topological classification of gapless structures. p is the codimension of a gapless structure. There are totally ten distinct topological classes in which the topological charges have 8-fold periodicity with respect to codimensions of the gapless structures. The topological charges are defined as same as those in Table. 1. Table. 2 is reproduced with permission from [95]. Copyright 2013, American Physical Society.

	Symmetry			p							
Class	T	C	S	1	2	3	4	5	6	7	8
A	0	0	0	$\mathbb{Z}$	0	$\mathbb{Z}$	0	$\mathbb{Z}$	0	$\mathbb{Z}$	0
AIII	0	0	1	0	$\mathbb{Z}$	0	$\mathbb{Z}$	0	$\mathbb{Z}$	0	$\mathbb{Z}$
AI	+1	0	0	0	0	$2\mathbb{Z}$	0	$\mathbb{Z}_2$	$\mathbb{Z}_2$	$\mathbb{Z}$	0
BDI	+1	+1	1	0	0	0	$2\mathbb{Z}$	0	$\mathbb{Z}_2$	$\mathbb{Z}_2$	$\mathbb{Z}$
D	0	+1	0	$\mathbb{Z}$	0	0	0	$2\mathbb{Z}$	0	$\mathbb{Z}_2$	$\mathbb{Z}_2$
DIII	-1	+1	1	$\mathbb{Z}_2$	$\mathbb{Z}$	0	0	0	$2\mathbb{Z}$	0	$\mathbb{Z}_2$
AII	-1	0	0	$\mathbb{Z}_2$	$\mathbb{Z}_2$	$\mathbb{Z}$	0	0	0	$2\mathbb{Z}$	0
CII	-1	-1	1	0	$\mathbb{Z}_2$	$\mathbb{Z}_2$	$\mathbb{Z}$	0	0	0	$2\mathbb{Z}$
C	0	-1	0	$2\mathbb{Z}$	0	$\mathbb{Z}_2$	$\mathbb{Z}_2$	$\mathbb{Z}$	0	0	0
CI	+1	-1	1	0	$2\mathbb{Z}$	0	$\mathbb{Z}_2$	$\mathbb{Z}_2$	$\mathbb{Z}$	0	0

Considering the combinations between T and other symmetries such as the inversion symmetry P, classification of gapless structures with respect of combined PT and CP symmetries was provided in [98]. Since the classification is based on the single-particle systems, it can be directly applied in the photonic system and offer new approached on finding various topological gapless phases.

Optics EXPRESS

3.2 Topological gapless photonic crystals

The gapless structures in PC have a significant influence on the transport properties of the bulk. For instance, the transmission of the PC at the frequency of gapless points will have a decay rate inversely proportional to the distance [99]. In terms of different dimensions, the gapless structures can be divided into gapless points, gapless nodal lines, and gapless surfaces.

3.2.1 Topological gapless points in PCs

Although the gapless points (GPs) in PC have been discovered in the very early work [27] where there are two gapless Dirac points (DPs) with linear dispersion at the Brillouin zone corners in the 2D hexagonal lattice, the topological properties of GPs themselves are not well studied. With defined basis, a typical Hamiltonian which describes the physics around the DPs is:

$$H_{DP} = v(q_x\sigma_x + q_y\sigma_y) \tag{10}$$

where v is the expansion coefficient and $\mathbf{q} = (q_x, q_y, q_z)$ is the momentum displacement from the gapless point. $\sigma_x, \sigma_y, \sigma_z$ are three Pauli matrices. These Dirac points in 2D are protected by PT symmetry and characterized by a $\mathbb{Z}_2$ topological charge according to the classification of gapless structures with respect to PT symmetry [27, 98]. One can consider a PC where P and T symmetries are individually broken down but with PT symmetry, then the gapless points still exist. Moreover, two gapless points are connected with a Fermi arc at the boundary of BZ which can be seen in the projected band structures. The Fermi arc [100] can be understood in following way: If we cut the 2D system in momentum space along a certain line, we can regard the system along this line as a 1D TI. For the line located between two topological gapless points with different topological charges, the 1D system along the line have non-trivial boundary states which located at the BZ boundary of 2D PC. However, if we move the 1D system to cross the gapless point in momentum space, there is a topological phase transition happened and the gapped 1D chain becomes topologically trivial. The collection of the gapless endpoint forms a 1D gapless structure which is the Fermi arc.

In 3D, there is another kind of gapless point which is the Weyl point (WP) [101–104]:

$$H_{WP} = v(q_x\sigma_x + q_y\sigma_y + q_z\sigma_z) \tag{11}$$

Different from DP, the Hamiltonian of WP uses all three Pauli matrices and therefore cannot be gapped out by adding any terms. This means that WPs do not need any symmetry protection and are more stable than DPs. They can only disappear by merging two WPs with different chiralities into each other. Consequently, WPs always emerge and disappear in pairs which is guaranteed by the Nielsen-Ninomiya theorem [105].

The first theoretical realization of WPs in PC is proposed by Lu [106]. The 3D PC consists of double-gyroid (DG) structures with a threefold degeneracy at BZ center as shown in Fig. 5(a). By putting air-sphere on two gyroids, or applying a d.c. the magnetic field, P symmetry, and T symmetry is broken respectively, and WPs emerge as shown in Fig. 5(b). For WPs with different chiralities, there are Fermi arcs connecting them. Later, several theoretical and experimental studies on WPs in PC appear in [107–117]. However, in DG PC, the WPs are isolated in frequencies which may put restraints on the applications. Recently, proposed by Yang et al. [118] a PC with Weyl points which have the same frequencies and are separated from any other bands is experimentally realized as shown in Fig. 5(c)-(d). The helicoid Riemann surface states as shown in Fig. 5(e) are also studied as the topological surface states of WPs.

Optics EXPRESS

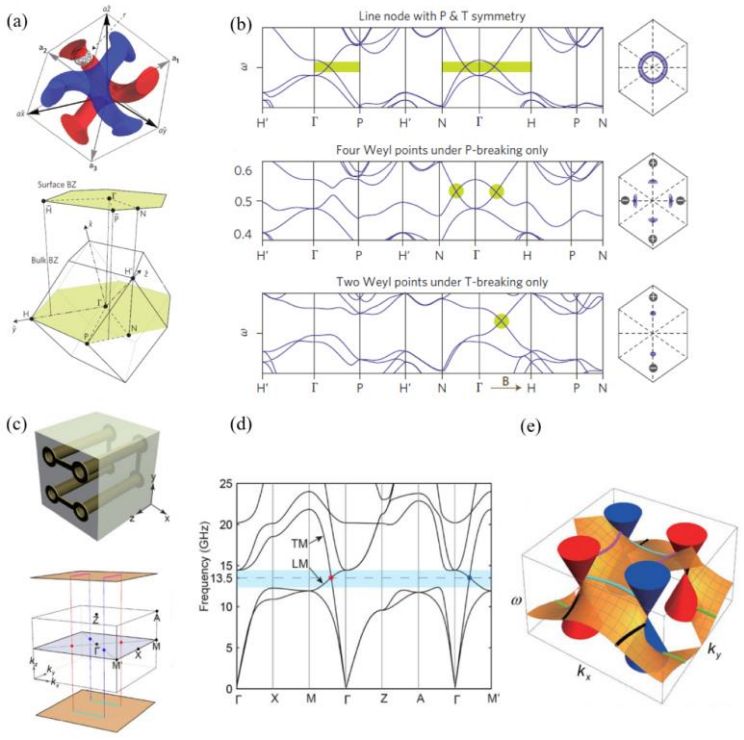

Fig. 5. WPs in PCs. (a). Double-gyroid (DG) structure of PC and the Brillouin zone (BZ). A sphere defect may be introduced in the structure to break T or P symmetry. (b). Band structures along a certain path in BZ of PC with different symmetries. The Weyl points (WPs) appear when P or T symmetry is broken. (c). Schematic of a saddle-shaped metallic inclusion and its BZ with WPs and surface-state arcs. (d). Band structures with ideal WPs. (e). Helicoid surface states plotted using Jacobi elliptic function. The arcs with different colors represent the evolution of equi-frequency arcs which connect WPs with opposite chirality. (a)-(b) are reprinted with permission from [106]. Copyright 2013, Springer Nature. (c)-(e) are reprinted with permission from [118]. Copyright 2018 Springer Science

So far, the group velocities of two bands near WPs have different signs. However, it is possible to have WPs with two bands having the same group velocity which are the type-II WPs [117, 119]. With the increase of symmetry, multi-WPs can appear at the high-symmetry points in BZ [114, 116]. Besides the robust WPs, DPs [69, 83] can also appear in 3D which are protected by discrete symmetries. As pointed by Wang et al. there are type-II DPs protected by non-symmorphic screw symmetry which are the mother states of type-II WPs [120]. Additionally, in another work [121], it is pointed out that DPs can emerge and be protected by point group symmetry.

3.2.2 Higher-dimensional topological gapless structures

In previous sections, we have investigated the gapless point structures in momentum space which have zero dimensionality. A natural extension of topological gapless structures to higher dimensionalities in PCs have also been proposed and explored. As an example, in 3D electronic materials and PCs, the 1D gapless structures which are lines with different shapes have been proposed [122–131]. Furthermore, in electronic materials, for a 1D gapless bulk structure with different topological charges, the topological surface states which connect them are 2D states such as the drum-head states [132]. The 2D gapless structures such as the nodal surfaces which are protected by screw rotations and T symmetry are explored in [133].

Optics EXPRESS

4. Other topological phases in photonic crystals

4.1 Topological non-Hermitian photonic crystals

Previously, we reviewed the studies of topological phases in Hermitian photonic systems in which the effective Hamiltonians are Hermitian matrices. However, if gain and loss of optical materials are considered, non-Hermiticity [134] is introduced in PCs [135, 136]. The emergent exceptional points [137] and exceptional rings in non-Hermitian PC have been studied in [138–142]. However, the topological properties in them were not well understood, especially in photonics. Recently, the topological band theory for non-Hermitian systems has been proposed [143–149]. Non-Hermitian Chern number, as well as another topological invariant which is the vorticity of the energy eigenvalues, were defined. The latter one has no counterpart in Hermitian systems which may introduce new topological phases. Gapless structures in non-Hermitian systems such as the non-Hermitian Weyl exceptional ring [142] have been theoretically proposed. The topological surface arcs connecting different Weyl exceptional rings with different topological charges may be very different from the Hermitian case [150].

4.2 Higher-order topological phases in photonic crystals

Conventionally, dD TI has dD gapped bulk states and (d-1)D gapless boundary states. Recently, the concept of higher-order topological insulator (HOTI) [151–156] has been put forward to describe those TIs which have lower-dimensional gapless boundary states. Generally speaking, an nth-order TI is defined as a dD TI with (d-1)D, (d-2)D, …, (d-n-1)D gapped boundary states and (d-n)D gapless boundary states. For example, a second-order TI (SOTI) in 2D has gapped 2D bulk states and 1D boundary states. However, the 0D boundary states which are called corner states is gapless. The HOTIs broaden the family of non-trivial topological insulating phases.

Originally, HOTI is thought to be realized in photonic systems with negative couplings which are not easy to be included [154]. Recently proposed by Xie et al. [157], a second-order photonic topological insulator (SOPTI) can be realized by all-dielectric materials and simple structures with corner states as shown in Fig. 6. Moreover, controllable quasi-1D topological edge states which appear only in opposite directions are found which may be used to design topological switch between SOTI and topological crystalline insulators [158]. A similar work of SOPTI which is in the hexagonal lattice is reported as a PTI with topological defect modes [159].

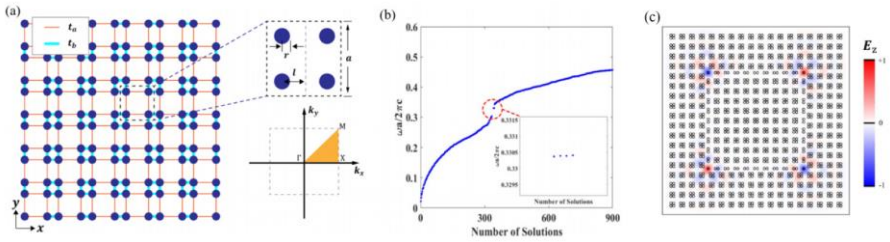

Fig. 6. Second-order photonic topological insulator with corner states. (a). Schematic of the PC and its Brillouin zone. (b). The eigenmodes of a square supercell as shown in (c). There are four degenerate states in the middle of the PBG. (c). Corner states which are strongly localized. (a)-(c) are reprinted from [157].

4.3 Geometric phase and measurement of topological invariant in photonic crystals

The topological properties of single-particle systems are characterized by the geometric phase such as Berry phase and Zak phase. As a photon goes around the Brillouin zone, beside the dynamical phase, it also acquires a phase on the wavefunction which is determined by the geometry and spin which have a non-trivial influence on the equation of motion [160]. Several experiments on measurements of geometric phase and topological invariant have

Optics EXPRESS

been proposed [161] and given [162, 163]. The gapless structures with non-trivial topological charges can be regarded as momentum-space magnetic monopoles. Direct measurement of topological charge of the gapless structures by using Aharonov-Bohm (AB) interferometer is presented in the cold-atom system [164] and photonic system [165]. The photonic analog of momentum-space AB effect is waiting to be found in the experiment.

5. Conclusions and outlooks

In previous sections, we briefly reviewed the exploration of various topological phases in photonic systems. The topological phases of single-particle Hermitian Hamiltonian can be divided into topologically gapped phases and topologically gapless phases. Starting from the topological classification, different implementations of topological phases with unique topological invariants were presented. Moreover, we revealed the relation between a variety of topological phases and discrete symmetries. To conclude, we would like to point out that the topology in photonics manifests itself in many different aspects including but not limited to previous contents. In future studies, a couple of topics about the topological photonics should be focused.

First and foremost, since the topological band theory are based on the single-particle description which can be well described by K-theory [166], if we consider the interaction between particles such as the many-body effect in condensed matter physics, new topological phases appear which may be described by the topological quantum field theory (TQFT) [167]. Classification of topological phase in interacting bosons has been developed by Wen et al [168]. In photonic systems, in order to introduce an interaction between photons, nonlinearity [169] should be considered. Recently, a three-body interaction and Pfaffian states have been realized in circuit-QED systems in [170]. We expect more discoveries of topological phases in interacting photonics which beyond the description of single-particle topological band theory.

Moreover, non-hermiticity induced topological phases in photonics are waiting to be explored. In photonic systems, the non-hermiticity is introduced by including gain and loss materials which is much easier to realize than introducing non-hermiticity in electronic materials. Therefore photonic systems provide us with convenient platforms to testify newly proposed non-Hermitian topological band theory [143]. More importantly, the topologically protected edge states with frequencies possessing positive imaginary parts may be used to design topological lasers [148, 149].

The topological properties are closely related to the geometry of the systems. The curvature of space and time have a non-trivial influence on the propagation of photons [171–174], for instance, introducing synthetic gauge fields [175]. In a very recent work [176], a 1-dimensional curved metamaterial with tunable spin-dependent geometric phase has been investigated. Due to the gauge freedom, the Rindler beam in general relativity has been generated. With the conveniences of easily controlled geometric structures in photonic systems, we expect more explorations on the topological photonics in curved space-time in future.

Funding

National Key R & D Program of China (Grant No. 2018FA0306202, 2017YFA0303700, 2018YFA0306200,); National Natural Science Foundation of China (NSFC) (Grant No. 51721001); Academic Program Development of Jiangsu Higher Education (PAPD); GRF of Hong Kong (Grants No. HKU173309/16P, No. HKU173057/17P).